



# Dual-Fibre Bragg Grating Sensor for Simultaneous Temperature and Strain Sensing of Composite Materials Manufacturing

Emmanuel Marin, Youcef Ouerdane

## ► To cite this version:

Emmanuel Marin, Youcef Ouerdane. Dual-Fibre Bragg Grating Sensor for Simultaneous Temperature and Strain Sensing of Composite Materials Manufacturing. EWSHM - 7th European Workshop on Structural Health Monitoring, IFFSTTAR, Inria, Université de Nantes, Jul 2014, Nantes, France. hal-01021254

**HAL Id: hal-01021254**

**<https://inria.hal.science/hal-01021254>**

Submitted on 9 Jul 2014

**HAL** is a multi-disciplinary open access archive for the deposit and dissemination of scientific research documents, whether they are published or not. The documents may come from teaching and research institutions in France or abroad, or from public or private research centers.

L'archive ouverte pluridisciplinaire **HAL**, est destinée au dépôt et à la diffusion de documents scientifiques de niveau recherche, publiés ou non, émanant des établissements d'enseignement et de recherche français ou étrangers, des laboratoires publics ou privés.

## DUAL-FIBRE BRAGG GRATING SENSOR FOR SIMULTANEOUS TEMPERATURE AND STRAIN SENSING OF COMPOSITE MATERIALS MANUFACTURING

Emmanuel Marin and Youcef Ouerdane

*Université de Lyon, F-42023, Saint-Etienne, France - CNRS UMR 5516,  
Laboratoire Hubert Curien, F-42000, Saint-Etienne, Université Jean-Monnet de Saint-Etienne,  
France.*

emmanuel.marin@univ-st-etienne.fr

### ABSTRACT

The Optical Fibre Sensors (OFS)-based monitoring of a composite part during its manufacturing process is presented. The sensor is made of a dual grating, *i.e.* a standard FBG and a Long Period Grating (LPG) photo-written at the same location, which provides accurate temperature and strain measurements, as well as a good spatial resolution. By using the differences of sensitivities of each grating, this dual-sensor is able to discriminate and to determine accurately temperature and strain. The dual-sensor has been tested during the curing of a pure epoxy resin, and a composite part obtained by Liquid Resin Infusion (LRI) process. Such dual-grating sensor is also very promising for SHM of composite parts.

**KEYWORDS :** *Optical Fibre Sensor, Fibre Bragg Grating (FBG), Long Period Grating (LPG), Composite material.*

### INTRODUCTION

Composite materials are more and more used in many industrial sectors such as aircraft industry, automotive, marine, etc. This expansion is mainly related to their specific advantages: light weight, high fatigue resistance, etc. Often the manufacturing process of multi-ply composite panels remains difficult, and some defects may occur, as dry zones, internal stresses, etc. As specific features of these materials are strongly linked to the manufacturing process respect, it becomes mandatory to control process parameters as temperature, time duration and pressure.

OFSs are often considered as an alternative solution to localize and to quantify such parameters, particularly in applications where the information cannot directly be assessed. Due to their low intrusiveness, optical fibres can be easily embedded into composites material to perform in situ and real-time measurements. Some optical sensors have already been used to monitor epoxy resin curing through the measurement of some optical properties. These include sensors based on near-infrared spectroscopy (FTIR) [1], Raman spectroscopy [2], evanescent wave spectroscopy [3], or refractive index monitoring [4,5]. Other optical sensors have been dedicated to monitoring temperature and strain. Different technics are used to achieve these measurements like Brillouin Optical Time Domain Reflectometer (BOTDR) [6], Brillouin Optical Time Domain Analysis (BOTDA) [7], Raman Distributed Temperature Sensor (Raman DTS) [8].

Among these, FBG-based sensors can be considered as one of the most interesting candidates. Although it is a great advantage that FBG-based sensors are sensitive to several external factors, it is important to separate the thermal effect from the mechanical effect. So to do this, it is necessary to have well-conditioned system (*i.e.* with different sensitivities). Several techniques have been already reported using FBGs [9-11] or long period gratings [12]. It is also possible to combine two techniques, *e.g.* BOTDR and FBG [13], to take advantages of both.

In the following part, the principle of the sensor is detailed, along with the experimental configuration. The experimental set-up required for curing the resin and for the LRI process is then described. Lastly, the results obtained with the embedded sensor during the curing of a pure epoxy resin, as part of the LRI process are presented and discussed.

## 1 EXPERIMENTAL

### 1.1 Dual grating Sensor principle

The sensor consists in an association of one FBG and one Long Period Grating (LPG). A standard FBG is obtained by photo-writing a refractive index modulation of half-micron period  $\Lambda$  in the core of a single mode optical fibre. On one hand, the FBG acts as a narrow band-pass reflection filter at a specific wavelength:

$$\lambda_{BF} = 2n_{eff}\Lambda \quad (1)$$

where  $n_{eff}$  is the effective index of the propagating core mode.

On the other hand, the Long Period Grating (LPG) has a higher period, typically a few hundred microns, which promote coupling between the propagating core mode and co-propagating cladding modes. The attenuation of the cladding modes results in the transmission spectrum containing a series of bands, corresponding to the coupling to a different cladding mode, centred at discrete wavelengths:

$$\lambda_{BL} = (n_{eff} - n_{eff\_clad})\Lambda \quad (2)$$

where  $n_{eff\_clad}$  is the effective index of the propagating cladding mode.

So, any change in the parameters of Equations (1) and (2), induced for example by a change in temperature or strain, shifts the Bragg wavelength.

It is assumed that, in appropriate ranges, the variation of the resonance wavelength  $\lambda_B$  is linear with strain and temperature:

$$\Delta\lambda_B = K_\varepsilon\Delta\varepsilon + K_T\Delta T \quad (3)$$

where  $K_\varepsilon$  and  $K_T$  are respectively the strain and temperature sensitivities,  $\Delta\varepsilon$  and  $\Delta T$  are respectively the variations of the longitudinal strain and the temperature applied to the grating. It is supposed at this stage that the strain field around the sensor is isotropic and homogeneous. From Equation (3), it is clear that two equations are needed to calculate the unknown parameters. For this purpose, a sensor formed of two superimposed fibre gratings (FBG and LPG) was developed. The two resonance wavelengths shift with different variations of strain and temperature, and thus the relation between  $\Delta\lambda_{BL}$  (for the LPG),  $\Delta\lambda_{BF}$  (for the FBG), temperature and strain can be expressed as:

$$\begin{bmatrix} \Delta\lambda_{BL} \\ \Delta\lambda_{BF} \end{bmatrix} = \begin{bmatrix} K_{\varepsilon L} & K_{TL} \\ K_{\varepsilon F} & K_{TF} \end{bmatrix} \begin{bmatrix} \Delta\varepsilon \\ \Delta T \end{bmatrix} = [K] \begin{bmatrix} \Delta\varepsilon \\ \Delta T \end{bmatrix} \quad (4)$$

where  $K_{\varepsilon F}$  ( $K_{\varepsilon L}$ ) and  $K_{TF}$  ( $K_{TL}$ ) are respectively the strain and the temperature sensitivities of the FBG (LPG). It is assumed that cross sensitivities can be neglected, as it has been demonstrated experimentally [14]. It has been proven that the sensitivities of LPG and FBG are different [15], and therefore solution to Equation (4) exists because the determinant of matrix  $[K]$  is not zero. Once the sensitivity coefficients are estimated by experimental calibrations, the applied variation of strain and temperature can be deduced.

All the sensors were made with the same experimental protocol as that described in [14]. Gratings were inscribed in an H<sub>2</sub>-loaded Corning® SMF-28™ fibre with the help of the CW UV laser @ 244 nm. The LPG was first written with the point-by-point technique, and then the FBG was written over the entire length ( $\approx 12$  mm) of the LPG using the well-known phase-mask technique with no fibre disassembly. Finally, the component was stabilized by heat treatment at 180°C for 3 h to remove the unstable part of the grating. To determine the sensor sensitivities, a specific bench [14] was used to impose axial strain and/or temperature on the sensor. As an example, the sensitivity matrix of one of the superimposed LPG/FBG sensors that were developed is reported:

$$[K] = \begin{bmatrix} K_{\varepsilon L} = -0.217 \text{ pm}/\mu\varepsilon & K_{TL} = 39.3 \text{ pm}/^\circ\text{C} \\ K_{\varepsilon F} = 1.18 \text{ pm}/\mu\varepsilon & K_{TF} = 9.75 \text{ pm}/^\circ\text{C} \end{bmatrix} \quad (5)$$

The sensitivities of each grating are clearly different that involve high decoupling efficiency.

## 1.2 Materials and process

The processed composite part was made of glass reinforcement with an epoxy resin. The resin was a HexFlow® RTM6 from Hexcel™ Composites, which is a premixed epoxy resin specifically dedicated to liquid composite moulding processes and commonly used in the manufacturing of composite materials, mainly in the aeronautics industry.

Two types of device were used in this work: one for testing only the curing of the resin and a second for the whole LRI process. For the curing tests, the resin was put in a silicon mould with two small holes and a sealant to place the dual grating sensor, all of which was positioned in an oven. A micro-thermocouple with a 110  $\mu\text{m}$  wire diameter was also positioned in the vicinity of the optical sensor to validate and compare the results. Some studies (*e.g.* [16]) have reported the use of a single FBG and a thermocouple to discriminate temperature from strain during the composite manufacturing process and to determine residual strains. However, the device developed here seems to be an alternative way to avoid using an invasive (metal-based) thermocouple. In-situ acquisition was performed throughout the curing cycle.

For the LRI tests, the reinforcement was made with a non-crimp fabric glass fibre mat [0/-45/90/+45] of 1 mm thickness. Two mats of 200 x 200 mm<sup>2</sup> square were symmetrically stacked to obtain a 2 mm quasi-isotropic composite plate part. In this case, the optical sensor was positioned in the symmetry plane of the glass preform. Like in pure resin cure tests, a thermocouple was also embedded near the optical sensor for comparison. The stacked preform was placed on an aluminium plate of 3 mm in thickness used as a mould.

The mould was treated with a release agent before to place the preform. Sealant was added around the preform with a permeable draining fabric and a vacuum bagging film placed on the top of the preform. Before infusion, the resin was preheated to 80°C in a heating chamber, connected to the vacuum bag inlet on one side, in order to decrease its viscosity and to make the infusion and the wetting of the glass fibre reinforcement easier. The liquid resin flow was then induced across the compressed preform thickness, also preheated to 80°C, as a result of a prescribed vacuum pressure over the preform created by a vacuum pump connected to the vacuum bag outlet. After infusion of the preform by the resin, a second heating was applied up to 150°C, followed by an isothermal curing phase of 120 min and, finally, by cooling to room temperature.

## 2 RESULTS AND DISCUSSION

The optical-grating-based sensor is used in two configurations: the monitoring of the resin curing alone and the LRI-process monitoring.

### 2.1 Pure resin curing monitoring

In a first application, the LPG/FBG sensor was embedded in a Hexcel RTM6 resin for the purpose of monitoring the curing process. Figure 1 presents the temperature (measured by the thermocouple embedded near the optical sensor for comparison) and the FBG and LPG wavelength shifts with time for the applied thermal cycle. The results shown in Figure 1 may be divided into three very distinct phases: the temperature increase (up to  $t_1$ ), the reticulation phase (cure plateau) from  $t_1$  to  $t_4$ , and the temperature decrease.

During the second phase (the cure plateau generally associated with the reticulation phase), two distinct thermal states can be observed. The first is an overshoot of the temperature from  $t_1$  to  $t_3$  which corresponds to the exothermal manifestation of chemical bonding, while the second state can be considered as isothermal at 130°C from  $t_3$  to  $t_4$ . However, in most cases studied, the overshoot does not appear to be as high as it was in this experiment. This difference can be explained, firstly by our use in this case of only pure resin, without reinforcement (a material with low thermal conductivity), and secondly by the facilitation of temperature diffusion caused by the large heat flux exchanged between the sample and the metallic mould, a phenomenon that cannot occur in a silicon mould. However, it is worth pointing out that, contrary to metallic moulds, this kind of silicon mould allows free deformations during the whole curing cycle.

Obviously, in our experiment, the resin reticulation did not occur at a constant temperature. During the reticulation phase, the epoxy resin continuously changes from its liquid state to its reticulated state, which simultaneously fixes on the optical fibre and allows strain transfer [17], leading to a continuous change in the behaviour of the material surrounding the sensor. The total strain applied to the sensor is the sum of a mechanical part (resin chemical shrinkage) and a thermal part (increase and decrease in the temperature) in a material whose stiffness is time-dependent. This is highlighted by the negative wavelength shift for the FBG from  $t_2$  along with the positive wavelength shift for the LPG (because the strain sensitivity of the LPG is negative), as depicted on Figure 1.

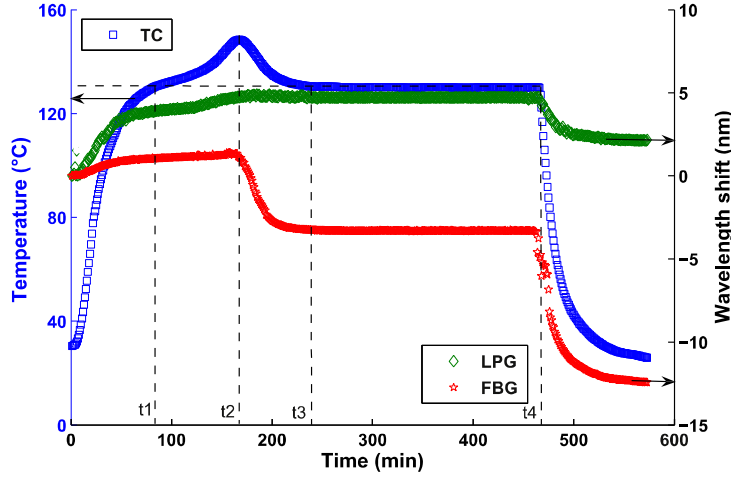


Figure 1: Thermocouple temperature (left), FBG and LPG wavelength shifts (right) vs. time recorded for the temperature cycle applied to the resin sample.

The curing ends after the plateau ( $t > t_4$ ), with the decrease in temperature, where the cure residual stresses are proportional to the measured residual strains [17]. In this case, the wavelength shift depends on strain and temperature. Under the hypothesis of a surrounding material volume considerably greater than the optical fibre volume (in such a case the effective behaviour of the assembly is essentially governed by the surrounding media [18]), it can be expressed as:

$$\Delta\lambda_B = K_\varepsilon\Delta\varepsilon + K_T\Delta T + K_\varepsilon(\alpha_{resin} - \alpha_{SiO_2})\Delta T = K_\varepsilon\Delta\varepsilon + K_T^*\Delta T \quad (6)$$

where  $\alpha_{resin}$  ( $\alpha_{SiO_2}$ ) is the thermal expansion coefficient of resin ( $SiO_2$ ).

The additional thermal-strain effect generally induces an increase in the temperature sensitivity, leading to the apparent temperature sensitivity, noted  $K_T^*$ , linked to the surrounding media.

From the curves of the FBG and LPG wavelength shifts, presented in Figure 1, and knowing the two temperature and the two strain sensitivities from calibration, as presented in Equation (5), discrimination can then be achieved. Figure 2-a shows the temperature response of our sensor (quoted FBG & LPG) during the curing cycle, while the total strain is reported in Figure 2-b. The results presented in Figure 2-a are validated by comparison with the thermocouple response for temperature (quoted TC). The results for the strain measurement presented in Figure 2-b are also validated by comparing the strain measured with our optical sensor and the strain deduced from the single FBG wavelength shift using the thermocouple to measure the temperature and to discriminate both factors. It is worth pointing out that these results are quite good, except for the temperature response during the overshoot, where the optical sensor and thermocouple responses differ slightly. This may be explained by the fact that the two sensors are not positioned strictly at the same location. These results and analyses suggest the following comments.

- The measured strain is not affected by the temperature variation up to  $t_2$
- Between  $t_2$  and  $t_3$  we observed a contraction of about  $3600 \mu\text{m/m}$  with a decrease in temperature of about  $20^\circ\text{C}$ . This is certainly the result of both the chemical contraction

coming from the resin reticulation and the thermal contraction induced by the resin surrounding the fibre during the decrease in temperature.

- Between  $t_3$  and  $t_4$  both strain and temperature are constant, which is consistent with the fact that there is no wavelength shift of both gratings, as seen in Figure 1.
- The temperature decrease and the strain from a thermal origin occur from  $t_4$ , following Equation (6). This thermal strain reaches about  $6500 \mu\text{m/m}$ . These large values can be explained by the fact that there are no reinforcement fibres.

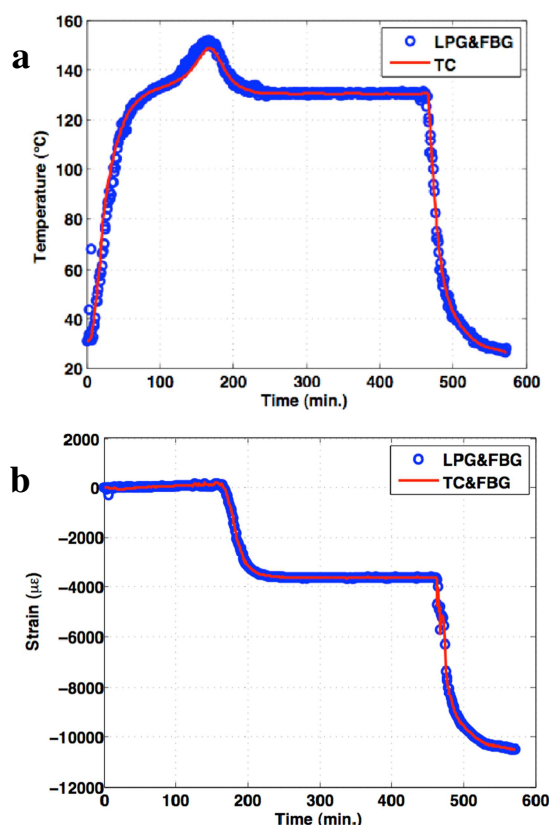


Figure 2: Temperature (a) and strain (b) measured with the superimposed LPG/FBG sensor during the pure resin curing process.

Finally, from Equation (6) the thermal expansion coefficient of the resin ( $\alpha_{resin}$ ) can be estimated by plotting the measured total strain with the temperature. The slope during the latter phase ( $t > t_4$ ) lead to a value of  $63 (\mu\text{m/m})/^{\circ}\text{C}$  for the thermal expansion coefficient of resin ( $\alpha_{resin}$ ), which is in good agreement with values from the literature [19].

## 2.2 Liquid Resin Infusion monitoring

As good results were obtained from sensor tests during the epoxy curing, the FBG/LPG sensor could now be embedded in a glass/epoxy (RTM6)-composite part made using the process of Liquid Resin Infusion (LRI), as previously described. Figure 3 reports the temperature measured by the thermocouple, along with the FBG and LPG wavelength shifts as a function of time during the whole process.

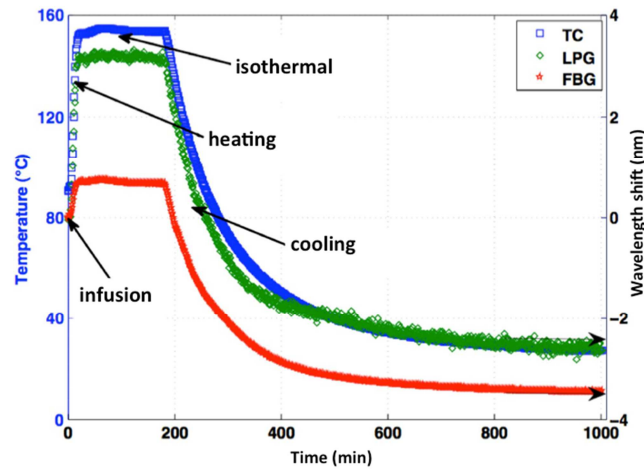


Figure 3: Thermocouple temperature (left), LPG and FBG wavelength shifts (right) during the LRI process.

From the raw wavelength-shift results shown in Figure 3, and with the sensitivity matrix, Equation (7), of optical-grating-based sensor obtained after the sensor calibration, discrimination of temperature and strain can then be achieved.

$$[K] = \begin{bmatrix} K_{\varepsilon L} = -0.266 \text{ pm}/\mu\varepsilon & K_{TL} = 50.9 \text{ pm}/^\circ\text{C} \\ K_{\varepsilon F} = 1.21 \text{ pm}/\mu\varepsilon & K_{TF} = 11 \text{ pm}/^\circ\text{C} \end{bmatrix} \quad (7)$$

Figure 4-a shows the temperature response of our sensor (quoted LPG & FBG) during the whole curing process, while the total strain is reported in Figure 4-b.

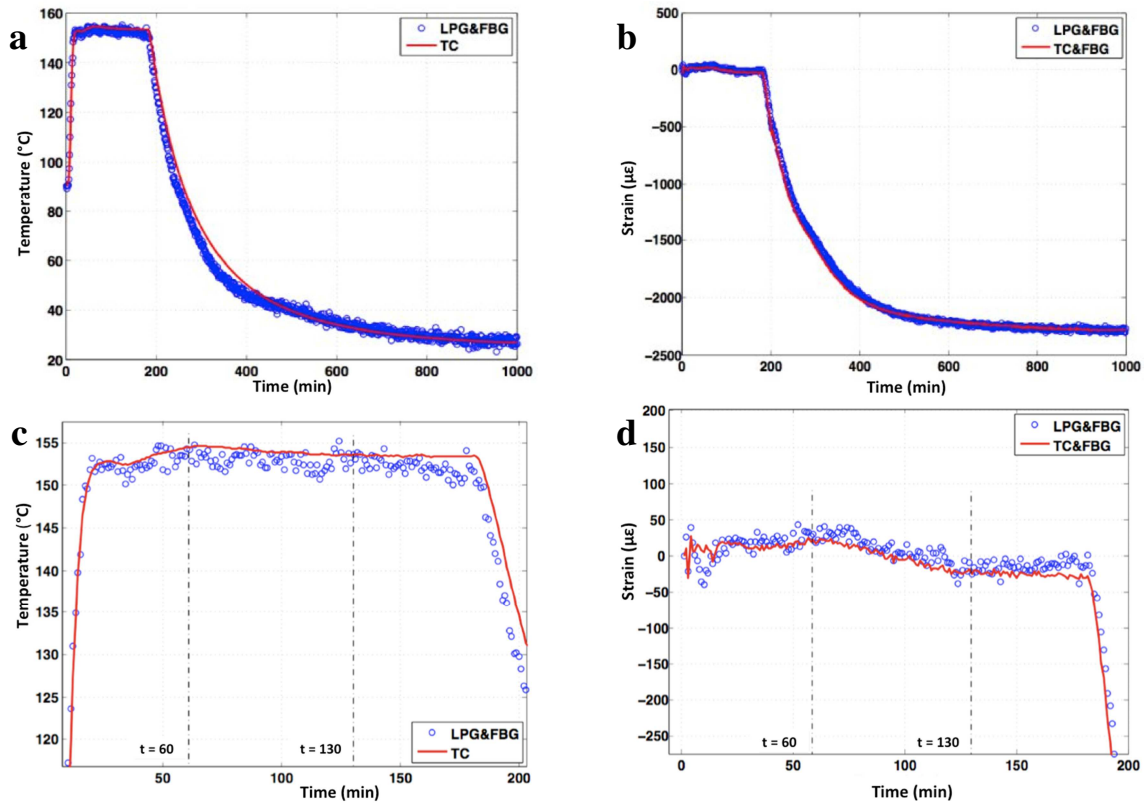


Figure 4: Temperature (a) and strain (b) measured with the superimposed LPG/FBG sensor during the LRI process. (c) and (d) are respectively the enlargement of (a) and (b).

The results presented in Figure 4-a are validated by comparing the thermocouple temperature response (quoted TC). Results for the strain measurement presented in Figure 4-b are also validated, by comparing the strain measured with our optical sensor and the strain deduced from the single FBG wavelength shift, using the thermocouple to measure the temperature and to discriminate between each factor (quoted TC & FBG). The enlargement of Figures 4-a and 4-b (presented in Figures 4-c and 4-d) highlights a decrease of about 100  $\mu\text{m/m}$  in the measured strain during the isothermal plateau ( $\Delta T = 0$ ). These results show that the measurable contraction starts at  $t = 60$  min and stops at  $t = 130$  min, demonstrating that the measured strains are coming from the chemical contraction of the epoxy resin.

After cooling, results for residual strains, which lead to cure residual stresses, can be calculated at 2250  $\mu\text{m/m}$  (see Figure 4-b). This value is lower than that reported for the pure epoxy resin curing because the coefficient of thermal expansion of the glass fibre is lower than that of the resin. In the case of a composite part provided by the LRI process, the measured strain coming from the chemical contraction of the epoxy resin is very weak, because it is prevented by glass reinforcement fibres. Thus, its detection remains difficult, contrarily to the case of curing pure epoxy resin. It is confirmed that the major share of residual stress in the reinforcement fibres is attributed to variations taking place at the time of the cooling-down phase, due to the mismatch between coefficients of thermal expansion and mould/ composite interactions.

## CONCLUSION

This paper describes the monitoring of a LRI composite manufacturing process. It focuses on the instrumentation of this process, which is carried out using an optical fibre sensor based on dual association of long and short period gratings. These were used to discriminate the temperature from the strain during the process. Our sensor was calibrated to obtain sensitivity responses before embedding, first in epoxy resin, then in a fibreglass/epoxy-composite part for LRI process monitoring.

The discrimination of the sensor temperature and strain responses was validated during a pure epoxy resin curing by comparing them with thermocouple measurements. The sensor presents an accurate monitoring response and low intrusiveness, while dispensing with the use of a thermocouple. Analysis of the curing allowed strains from chemical origins (shrinkage) and thermal origins to be assessed. The LRI process was also monitored with the superimposed grating sensor. The developed sensor presents a good and accurate response for the monitoring of such a process. In the case of LRI process, the optical-grating-based sensor has been also enough sensible to detect chemical contraction of the epoxy resin although this effect is reduced by the reinforcement.

As a consequence of these good results, we claim dual-FBG transducers are very good candidates to monitor composite structures life from their manufacturing process up to their end of life, including the SHM during their industrial use, providing crucial information for curing monitoring and quality control, but also for qualification, residual life time assessment, and maintenance scheduling.

## REFERENCES

- [1] T. Liu, G. Fernando, Processing of polymer composites: an optical fibre-based sensor system for on-line amine monitoring, *Comp. Part A: Appl. Sci. Manuf.* 32 (2001) 1561–1572.
- [2] L. Merad, M. Cochez, S. Margueron, F. Jauchem, M. Ferriol, B. Benyoucef, P. Bourson, In-situ cure monitoring using optical fibre sensors – a comparative study, *Polym. Test.* 28 (2009) 42–45.
- [3] G. Powell, P. Crosby, D. Waters, C. France, R. Spooncer, G. Fernando, In-situ cure monitoring using optical fibre sensors – a comparative study, *Smart Mat. Struct.* 7 (1998) 557–568.
- [4] S. Vacher, J. Molimard, H. Gagnaire, A. Vautrin, A Fresnel's reflection optical fiber sensor for thermoset polymer cure monitoring, *Polym. Comp.* 12 (4) (2004) 269–276.



- [5] V. Dewynter-Marty, S. Rougeault, P. Ferdinand, M. Bugaud, P. Brion, G. Marc et P. Plouvier, Quatre technologies de CFO pour le suivi de fabrication de matériaux composites, 19èmes Journées Nationales d'Optique Guidée (JNOG 1999), 6-8 déc. 1999, Limoges, France, pp. 67-69.
- [6] X.Y. Bao, 32 km Brillouin loss based distributed temperature sensor, presented at the 9th Opt. Fiber Sens. Conf., 1993.
- [7] T. Kurashima, T. Horiguchi, and M. Tateda, Distributed-temperature sensing using stimulated Brillouin-scattering in optical silica fibers, *Opt. Lett.*, vol. 15, no. 18, pp. 1038–1040, 1990.
- [8] J. P. Dakin, D. J. Pratt, G. W. Bibby, and J. N. Ross, Distributed optical fiber Raman temperature sensor using a semiconductor light-source and detector, *Electron. Lett.*, vol. 21, no. 13, pp. 569–570, Jun. 1985.
- [9] S. Magne, S. Rougeault, M. Vilela and P. Ferdinand, State-of-strain evaluation using fiber Bragg grating rosettes - Application to discrimination between strain and temperature effects in fiber sensors, *Appl. Opt.*, Vol. 36, n° 36, pp. 9437-9440, 1997.
- [10] M. Xu, J.-L. Archambault, L. Reeckie, J. Dakin, Discrimination between strain and temperature effects using dual-wavelength fibre grating sensors, *Elect. Lett.* 30 (13) (1994) 1085–1087.
- [11] H. K. Bal, F. Sidirolou, Z. Brodzeli, S. A. Wade, □G. W. Baxter and S. F. Collins, Temperature independent bend measurement using a pi-phase shifted FBG at twice the Bragg wavelength, Fourth European Workshop on Optical Fibre Sensors (EWOFS), Porto - Portugal, Proc. of SPIE Vol. 7653 76530H, 2010.
- [12] Y. Han, S. Lee, C.-S. Kim, J. Kang, U.-C. Paek, Y. Chung, Simultaneous measurement of temperature and strain using long period fiber gratings with controlled temperature and strain sensitivities, *Opt. Express* 11 (5) (2003) 476–481.
- [13] T. Yari, T. Shimizu, K.Nagai and N. Takeda, Structural health monitoring system for aerospace structures using optical fiber distributed sensor, Proc. 3<sup>rd</sup> Int. Workshop on Structural Health Monitoring, 2001, pp. 355-362.
- [14] S. Triollet, L. Robert, E. Marin, Y. Ouerdane, Discriminated measures of strain and temperature in metallic specimen with embedded superimposed long and short fibre Bragg gratings, *Meas. Sci. Tech.* 22 (2011) 015202.
- [15] V. Bhatia, Applications of long-period gratings to single and multi- parameter sensing, *Opt. Express* 4 (1999) 457–466.
- [16] M. Mulle, F. Collombet, P. Olivier, R. Zitoune, C. Huchette, F. Laurin, Y.- H. Grunevald, Assessment of cure-residual strains through the thickness of carbon-epoxy laminates using FBGs Part II: technological specimen, *Comp. Part A: Appl. Sci. Manuf.* 40 (2009) 1534–1544.
- [17] M. Mulle, F. Collombet, P. Olivier, Y.-H. Grunevald, Assessment of cure-residual strains through the thickness of carbon-epoxy lami- nates using FBGs Part I: elementary specimen, *Comp. Part A: Appl. Sci. Manuf.* 40 (2009) 94.
- [18] Y. Wang, B. Han, D.W. Kim, A. Bar-Cohen, P. Joseph, Integrated measurement technique for curing process-dependent mechanical properties of polymeric materials using fibre Bragg grating, *Exp. Mech.* 48 (2008) 107–117.
- [19] K. Magniez, A. Vijayan, N. Finn, Apparent volumetric shrinkage study of RTM6 resin during the curing process and its effect on the residual stresses in a composite, *Polym. Eng. Sci.* 52 (2) (2012) 346–351.